

# Relaxation Mechanisms and Effects of Motion in Albite ( $\text{NaAlSi}_3\text{O}_8$ ) Liquid and Glass: A High Temperature NMR Study

S.B. Liu<sup>1,2</sup>, A. Pines<sup>1</sup>, M. Brandriss<sup>2</sup>, and J.F. Stebbins<sup>2,3</sup>

<sup>1</sup> Department of Chemistry, University of California and Lawrence Berkeley Laboratory, Berkeley, CA 94720, USA

<sup>2</sup> Department of Geology, Stanford University, Stanford, CA 94305, USA

<sup>3</sup> To whom correspondence should be addressed

**Abstract.** The nuclear magnetic relaxation of  $^{23}\text{Na}$  and  $^{29}\text{Si}$  in albite glass and liquid has been studied from 800 K to 1400 K. The dominant spin-lattice relaxation mechanism for  $^{23}\text{Na}$  is found to be nuclear quadrupole interaction arising from the  $\text{Na}^+$  diffusion. The activation energy of the Na diffusion is found to be  $71 \pm 3$  kJ/mol, in close agreement with the results on electrical conductivity and on Na self-diffusion from radio-tracer experiments. The correlation time of the Na motion is estimated to be about  $8.5 \times 10^{-11}$  s near the melting point ( $\sim 1390$  K). Both nuclear dipole-dipole interaction and chemical shift anisotropy interaction are large enough to contribute to the  $^{29}\text{Si}$  relaxation. However, calculations based on a simplified model which employ single correlation time and exponential correlation function, with interactions typical of crystalline silicates, cannot completely account for the experimental data. NMR relaxation data also reveal that the Si motion is correlated to the Na motion and that the Si is relatively immobile. Several possible motions of  $\text{SiO}_4$  tetrahedra that can cause  $^{29}\text{Si}$  relaxation are suggested. The motion responsible for  $^{29}\text{Si}$  relaxation differs from that which is responsible for viscosity: the apparent activation energy for the former is much lower. Measurements of spin-spin relaxation times and linewidths are also presented and the significance of their temperature dependence is discussed.

## Introduction

Molten silicates play a fundamental role in many geological processes, and are involved in a wide variety of technologies, from glass making to metals extraction. As complex, difficult-to-study materials, they present great challenges to chemists in a number of fields.

The traditional basis of our present understanding of chemical and physical properties of molten silicates has been studies of the bulk thermodynamic and transport properties of the melts. Melts of albite ( $\text{NaAlSi}_3\text{O}_8$ ) composition have been frequently chosen, because of the abundance of this component in natural systems, its role as a "simple" analog for silica-rich, highly viscous magmas, its low melting point and its ease of glass formation. Recent work has included phase equilibrium studies (Boettcher et al. 1984), thermochemical measurements (Richet and Bottinga 1983, Stebbins et al. 1983, Rammensee and Fraser 1982, Navrotsky et al. 1982), viscometry (Urbain et al.

1982, Cranmer and Uhlmann 1981), and electrical and diffusion measurements (Jambon and Carron 1976, Jambon and Semet 1978).

Interpretation of macroscopic properties in terms of microscopic mechanisms has been based primarily on spectroscopic data of glasses at room temperature. Recent studies of albite glass by Raman spectroscopy (e.g. Sharma et al. 1978a, Mysen et al. 1980 and 1981, McMillan et al. 1982, Seifert et al. 1982, McKeown et al. 1984), by x-ray scattering (Taylor and Brown 1979), by EXAFS spectroscopy (McKeown et al. 1985a, b), and by  $^{29}\text{Si}$  MAS NMR (Kirkpatrick et al. 1985, Murdoch et al. 1985), lead to a picture of structure which retains a considerable degree of short-range order. The glass consists primarily of three-dimensionally connected  $\text{SiO}_4$  and  $\text{AlO}_4$  tetrahedra, mostly linked in six-membered rings. Sodium cations seem to play an interstitial, charge-balancing role as in crystalline feldspars. Cation-oxygen bond distances are similar to those in the crystal, but greater ranges of bond angles and second-neighbor coordinations are present.

Because a glass generally is assumed to retain the "quenched in" equivalent of the static liquid structure at the glass transition, study of the glass is a sensible starting point for understanding the liquid. Such a view is supported by a few spectroscopic studies on silicate melts at high temperature (Sharma et al. 1978b, Waseda 1980), which show that the local, static glass and melt structure are quite similar. The same may not be true for borosilicates (Furukawa and White 1981).

However, the thermodynamic properties of liquids are quite distinct from those of glasses: substantial increases in thermal expansion, compressibility, and heat capacity occur on transition from the glass to the liquid. At temperatures important in most solid-melt phase equilibria, these changes result in entropies, enthalpies, and molar volumes in the liquids which are significantly increased above the glass values. Determination of the structural and dynamical reasons for these differences is the subject of this paper.

The glass transition is generally considered to be the temperature ( $T_g$ ) at which, during cooling, structural relaxation in liquid can no longer keep pace with the cooling rate, and equilibrium with respect to some kind of structural motion can no longer be retained (e.g. Brawer 1985). On reheating, a relatively abrupt change (resembling in some ways a second order phase transition) occurs when structural rearrangement again becomes possible. Because constant volume heat capacities above  $T_g$  are generally considerably

higher than  $3R$  per gram-atom, the additional disorder generated above  $T_g$  is considered a contribution to the configurational entropy of the melt. The implied close relationship between flow, the glass transition, and thermodynamic properties has been emphasized recently by Richet (1984) and Richet et al. (1986), who have shown that theories relating viscosity and configurational entropy (Adam and Gibbs 1965, Gibbs and DiMarzio 1958) can be applied accurately to silicates.

The fundamental distinguishing feature of a liquid is that local relatively large scale motions can take place to allow flow and configurational change. Techniques such as vibrational spectroscopy, which sample the structure at a very short time scale, cannot reveal this kind of motion (Eisenberg and Kauzmann 1969). We therefore know very little about the mechanistic basis of the glass transition, or about the real causes of the properties which make silicate melt a liquid. *Nuclear magnetic resonance* (NMR) spectroscopy is, however, a potentially powerful tool to address these questions at the heart of the relationship between equilibrium and transport properties.

NMR has long been used to study low frequency motion in liquids, glasses, and molecular solids (reviewed in standard textbooks, such as Fyfe 1983, Slichter 1980, Farrar and Becker 1971, Abragam 1961). Several types of NMR experiments are relevant to silicate melts.  $^{29}\text{Si}$  NMR spectra of melts at a range of temperatures have shown, for example, that silicon atoms exchange rapidly among sites, beginning one or two hundred degrees above the glass transition (Murdoch et al. 1984, Schneider 1985, Stebbins et al. 1985). This kind of motion involves breaking and reforming of Si–O bonds and may be directly related to viscous flow.

Another, more general aspect of NMR makes it an even more powerful tool for studying motion. When a nucleus is excited to a high energy state by a *radio-frequency* (rf) pulse, the only important way that it can release that energy and return to equilibrium is through stimulated emission. This transfer of spin energy to random thermal energy is termed “spin-lattice relaxation” and the inverse of the relaxation rate is symbolized by “ $T_1$ ”. A dipolar nucleus (such as  $^{29}\text{Si}$ ) must therefore experience a fluctuating magnetic field at its resonant frequency in order to undergo this relaxation. A quadrupolar nucleus (such as  $^{23}\text{Na}$ ) can, in addition, couple to fluctuations in the local electric field gradient caused by motion of the atoms in the material. Measurement of relaxation times can therefore reveal a great deal about structural mobility.

A second type of nuclear relaxation is “spin-spin relaxation”, characterized by “ $T_2$ ”.  $T_2$  is a measure of how quickly the observed NMR signal decays, and is closely related to the inverse of the overall linewidth of the spectrum.  $T_2$  in liquids is usually close to or equal to  $T_1$ , but may be much shorter than  $T_1$  in solids and in viscous liquids where motional frequencies are too low to cause line-narrowing. Under these conditions, measurement of  $T_2$  can yield additional information about motion.

In this paper, we present the first NMR results collected for  $\text{NaAlSi}_3\text{O}_8$  glass and liquid at high temperature. We show that local-scale, atomic motion of both silicon and sodium cations are in some way closely related to the macroscopic glass transition. The relaxation data presented are a first step in understanding the details of how local motion changes at the glass transition, and how flow and change in structure occur in the liquid. Further results and interpre-

tations will be presented in a companion study of a series of alkali silicate and alkali aluminosilicate glasses and melts (Liu et al., submitted).

## Experimental Considerations

### Sample Preparation

Three samples of  $\text{NaAlSi}_3\text{O}_8$  glass were studied. One was prepared by melting a sample of an extremely pure natural albite ( $\text{Ab}_{100}$ , Neil and Apps 1979) for several h at  $1550^\circ\text{C}$ . A second sample was prepared from high-purity  $\text{Na}_2\text{CO}_3$ ,  $\text{Al}_2\text{O}_3$ , and  $\text{SiO}_2$ . The third sample was prepared using 95%  $^{29}\text{Si}$  enriched  $\text{SiO}_2$ . Both synthetic samples were heated at about  $1500^\circ\text{C}$  for several h, re-ground, and remelted until homogeneous. All three were confirmed to be crystal-free by optical and x-ray techniques. Stoichiometry was confirmed by careful monitoring of weight loss during sample preparation and by electron microprobe analysis.

High temperature NMR experiments were made with 0.5 to 0.7 g samples contained in crucibles made from hexagonal *boron nitride* (BN), blanketed by argon or argon with a small percentage of hydrogen. Run times were kept to a minimum (less than 1 h at the highest temperature) to minimize compositional change. Under comparable or more extreme conditions during sample synthesis, weight loss was not significant, and evaporation of Na should therefore be small during the actual NMR experiments (less than 0.5% absolute). A small amount of the borate binder in the crucible material did dissolve in the samples, however: analyses of the natural-abundance silicon samples after the experiments showed that they both contained about 0.4 weight percent  $\text{B}_2\text{O}_3$ .

Because of the potential importance of paramagnetic impurities in nuclear spin relaxation, the natural abundance silicon samples were also analysed for total Fe content, which was  $100 \pm 20$  ppm. The  $^{29}\text{Si}$  enriched glass, made from  $\text{SiO}_2$  originally containing less than 5 ppm Fe (data sheet from Oak Ridge National Laboratory), probably contained considerably less iron (most likely in the 10's of ppm range). However, the sample could not be analysed because of the great value of the isotope.

### High Temperature Apparatus

The high temperature apparatus consisted of several major components: the water jacket, the furnace and furnace power supply, and the NMR probe. The water jacket and the furnace design are similar to those reported earlier (Stebbins et al. 1986). The NMR probe used here is, however, designed specifically for relaxation time studies and is different from the shuttling probe described by Stebbins et al. (1986). With the previous design, the sample is shuttled between the furnace and rf coil which is located outside of the furnace. The disadvantages of using the shuttling probe design for relaxation studies are, first of all, the average shuttling time of 0.2 s limits the relaxation times that can be observed. Secondly, the abrupt change of sample temperature after the sample is shuttled from the furnace prevents accurate relaxation time and temperature measurements. In the new system, therefore, the rf coil and the sample are both fixed at the center of the furnace, as in the apparatus described by several other groups (e.g. Ploum-bidis 1979, Aurora and Day 1982, Soller et al. 1979).

The drawbacks of using the static probe design are the difficulties and inconveniences of dealing with high temperature materials, and the construction of the NMR probe. In particular, refractory metals used for the rf coil have relatively high electrical resistances, especially at high temperature, and hence a relatively low quality factor ( $Q$ ) electronic circuit results. In order to maximize the signal-to-noise ratio ( $S/N$ ), a solenoidal rf coil was used, and the sample container was designed to maximize the coil filling factor. In addition, careful cooling arrangements have to be made to provide thermal insulation between the furnace and the electronic components. The new probe used to collect the data presented here is about an order of magnitude more sensitive than the shuttling probe under comparable experimental conditions.

Typically, about 380 watts of DC power were required at a temperature near 1100° C. The temperature of the sample was measured using a Pt/Pt-10 percent Rh thermocouple placed roughly 3 mm above the sample. The actual sample temperature and temperature gradient have been calibrated with a second thermocouple temporarily placed inside a sample container. The temperature measurements reported here are accurate to  $\pm 5^\circ$  C.

### NMR Spectroscopy

All NMR measurements were recorded on a home-built NMR spectrometer operating at 4.2 Tesla, corresponding to a Larmor resonance frequency ( $f_0$ ) of 35.52 and 47.30 MHz for  $^{29}\text{Si}$  and  $^{23}\text{Na}$  respectively. The NMR probe consists of a solenoidal molybdenum rf coil and the tuning electronic circuits which can be adjusted remotely outside the magnet. The tank circuit gives a  $Q$  which is approximately 85 at room temperature but decreases to  $\sim 10$  at 1100° C due to the increase of resistance of the coil wire as temperature increases. This is, at present, the factor limiting data collection to below  $\sim 1200^\circ$  C. Typical  $\pi/2$  pulse length is 10  $\mu\text{s}$  for  $^{23}\text{Na}$  and 17  $\mu\text{s}$  for  $^{29}\text{Si}$  at room temperature.

The spin-lattice relaxation times ( $T_1$ ) were measured using the conventional saturation/recovery pulse sequence. The spin-spin relaxation times ( $T_2$ ) were obtained using  $(\pi/2)_x - \tau - (\pi)_y$  (Hahn spin echo) sequence (Hahn 1950). The NMR lineshapes and linewidths were obtained by Fourier transforming free induction decay (FID) signals or spin echoes. Typically, 50 to 100 FIDs (or spin echoes) were accumulated.

## Experimental Results

### $^{23}\text{Na}$ Relaxation Times

The  $^{23}\text{Na}$  nuclear relaxation times ( $T_1$ ,  $T_2$ ) of both natural and synthetic albite glass and liquid are shown in Figure 1 as a function of reciprocal temperature.

The  $T_1$  data from the two samples agree well and have the same temperature dependence as the  $T_2$  data from the synthetic albite sample. The temperature dependence of the relaxation data agrees with the results of linewidth study and can be described by an Arrhenius relation (see below):

$$\tau = \tau_0 \exp(-E_a/kT), \quad (1)$$

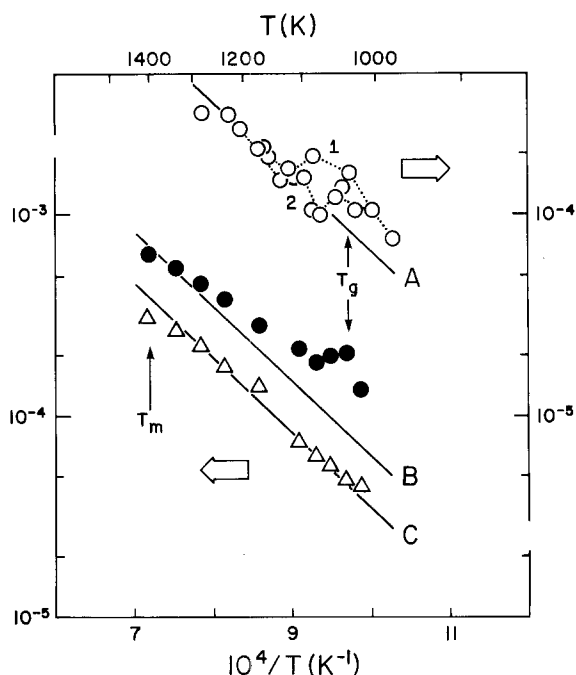


**Fig. 1.** NMR relaxation times ( $T_1$ ,  $T_2$ ) of  $^{23}\text{Na}$  in  $\text{NaAlSi}_3\text{O}_8$  glass and super-cooled liquid as a function of reciprocal temperature. The vertical scales are in seconds. A: Spin-lattice relaxation times  $T_1$  (scale at right) for sample derived from natural albite. Data on curve 1 were collected on initial heating, data on curve 2 on a second heating.  $T_g$  is the macroscopic glass transition temperature typically seen in an annealed sample (Arndt and Haberle 1973), and  $T_m$  is the melting point of the crystal. B:  $T_1$  data for a synthetic albite glass sample (scale at left). The scale of B (and C) is offset from A by one decade; A and B are the same within error if the two sets of data are not offset. C: Spin-spin relaxation times  $T_2$  for the same sample as B, plotted on the same scale as B. Straight lines A and B are identical when plotted together, but C is slightly offset. All are drawn with the same slope as the fit to the linewidth data shown in Figure 3

where  $\tau_0$  is the exponential pre-factor,  $E_a$  is the activation energy and  $k$  is the Boltzmann constant.

The temperature range in the data for  $\text{NaAlSi}_3\text{O}_8$  was not great enough to observe the  $T_1$  minima that were seen for both  $^{23}\text{Na}$  and  $^{29}\text{Si}$  in alkali silicate glasses (Liu et al., submitted). As described under "Discussion" below, spin lattice relaxation is caused by fluctuations in the local magnetic field or electric field gradient at the Larmor frequency of the nucleus. These fluctuations are typically caused by atomic or molecular motion at frequencies much lower than those of typical inter-atomic vibrations. At low temperatures, these frequencies are too low for efficient relaxation, and  $T_1$  values are long. At high temperatures, average motional frequencies are much greater than the Larmor frequency, and relaxation is again inefficient and slow. At intermediate temperatures, a minimum in  $T_1$  is often produced. For  $^{23}\text{Na}$  in  $\text{NaAlSi}_3\text{O}_8$  liquid, the slope in Figure 1 shows that all of our data must be at temperature higher than this minimum, which probably lies at about 900 K.

Distinct  $T_1$  anomalies were seen for both samples near the glass transition temperature, as determined by thermal expansion measurements (Arndt and Haberle 1973). For the natural albite sample, the  $T_1$  anomaly peak moved to

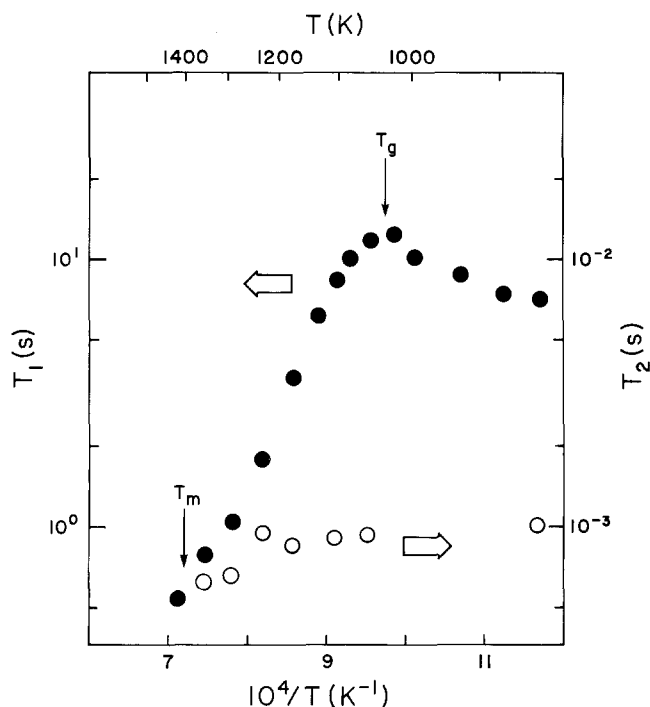


**Fig. 2.**  $^{29}\text{Si}$   $T_1$  (solid circles, left scale) and  $T_2$  (open circles, right scale) for a  $^{29}\text{Si}$ -enriched synthetic albite glass sample. Axes and symbols as in Figure 1

lower temperature as the sample was annealed. This is indicated in Figure 1 by curves 1 and 2.

### $^{29}\text{Si}$ Relaxation Times

Relaxation times  $T_1$  and  $T_2$  of synthetic  $^{29}\text{Si}$ -enriched albite glass ( $\text{NaAl}^{29}\text{Si}_3\text{O}_8$ ) are shown in Figure 2. The  $^{29}\text{Si}$   $T_1$  values are approximately three to four orders of magnitude longer than those for  $^{23}\text{Na}$  and have a markedly different temperature dependence.

Below  $T_g$ ,  $T_1$  increases with increasing temperature. At  $T_g$ , an abrupt change to the opposite slope is seen, suggesting a change of relaxation mechanism. For  $T > T_g$ ,  $T_1$  decreases as temperature increases. No  $T_1$  minimum is observed up to the maximum temperature of the measurements. The temperatures are therefore below the  $T_1$  minimum for the high temperature relaxation. We note that the  $^{29}\text{Si}$   $T_1$  minimum, if observed, will be several hundred degrees higher than the expected  $^{23}\text{Na}$   $T_1$  minimum. This suggests that Si is relatively immobile compared to Na, as expected from other studies of transport properties. Similar behavior is observed for all alkali silicate liquids examined in this laboratory (Liu et al., submitted) and is considered as a common signature of molten alkali silicates. In addition, the  $T_1$  curve above  $T_g$  shows a slight curvature away from Arrhenius behavior.

In contrast, the  $^{29}\text{Si}$   $T_2$  data are temperature independent below 1250 K. This behavior is frequently seen in molecular solid and liquids, especially in the low temperature limit where the correlation time  $\tau_c$  for the motion responsible for line-narrowing (see below) is much longer than  $T_2$ , and is usually referred as the "rigid lattice" limit (Abragam 1961). At  $T > 1250$  K,  $T_2$  begins to decrease with increasing temperature; this correlates well with the beginning of line narrowing (see below).

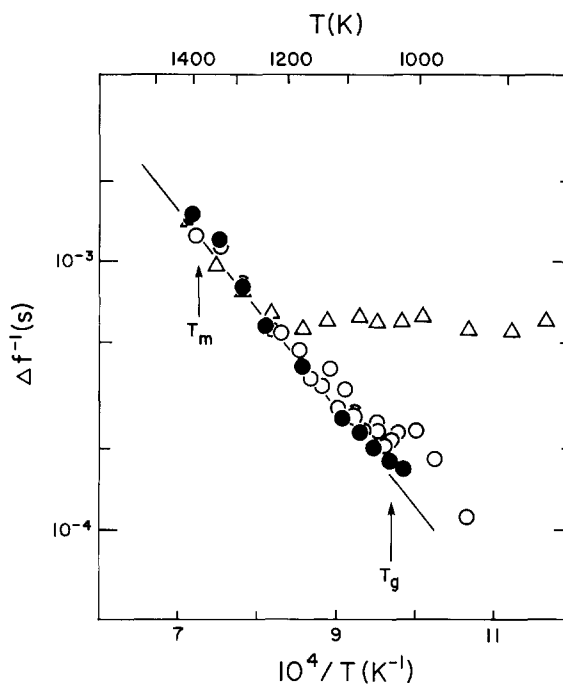


**Fig. 3.** The inverse of full width half-intensity linewidth plotted against reciprocal temperature. Open triangles:  $^{29}\text{Si}$  data. Open circles:  $^{23}\text{Na}$  data for sample derived from natural albite. Solid circles: synthetic albite glass. Other symbols as in Figure 1. Note coincidence of all three data sets at high temperature. The straight line indicates a fit to Arrhenius relation (Equation 1), and give an activation energy  $E_a = 71 \pm 3$  kJ/mol. The same slope is also indicated by solid lines A, B, and C in Figure 1

### Linewidth Study

The inverse linewidth data ( $\Delta f^{-1}$ ) for  $^{29}\text{Si}$  and  $^{23}\text{Na}$  (full width and half-maximum intensity or FWHM) are plotted against reciprocal temperature in Figure 3.

The  $^{23}\text{Na}$  linewidths of the natural and synthetic sample agree very well and have the same temperature dependence as the  $T_1$  data in Figure 1. The straight line in Figure 3 indicates a fit according to equation (1) and gives an activation energy of  $71 \pm 3$  kJ/mol. The same slope is also shown in Figure 1 by the three solid lines A, B and C. Furthermore, an anomaly of linewidth measurements near  $T_g$  is also seen, as observed in the  $T_1$  data. At high temperatures, where lineshapes close to a Lorentzian were observed, the experimental value of  $\Delta f^{-1}/T_2 \approx 3.2$  is almost identical to the expected theoretical ratio  $\Delta f^{-1}/T_2 = \pi$  (Boden 1979).

The  $^{29}\text{Si}$  linewidth is temperature independent for  $T < 1250$  K, in agreement with the  $T_2$  results in Figure 2. For  $T > 1250$  K, it is surprising that the  $^{29}\text{Si}$  linewidths are almost identical to the  $^{23}\text{Na}$  linewidths. It is not clear whether the temperature dependence of linewidth and  $^{29}\text{Si}$   $T_2$  data are related to the slight change of slope of  $^{29}\text{Si}$   $T_1$  data above 1250 K.

### Discussion

NMR relaxation times provide information on the structure as well as the dynamics of silicate melts. The standard first step at quantifying these relationships is based on the theory presented by Bloembergen, Purcell, and Pound (BPP) in 1948. They showed that fluctuating magnetic fields or elec-

tric field gradients arising from random molecular motions are directly related to the relaxation processes in liquids. The duration of the fluctuating local field is usually characterized by the correlation time  $\tau_c$ . For small molecules in typical non-viscous liquids, random isotropic motion in a given time  $\tau$  can be described by a single correlation time and exponential correlation function  $G(\tau) = G(0)\exp(-\tau/\tau_c)$ .

The energy of interaction that is modulated by the molecular motion may give rise to a distribution of frequencies which is the Fourier transformation of  $G(\tau)$  and is called the spectral density  $J(\omega)$ ;  $J(\omega)$  is proportional to  $\tau_c/(1 + \omega_0^2 \tau_c^2)$ , where  $\omega_0 = 2\pi f_0$ , and  $f_0$  is the Larmor resonant frequency in Hz. The spin-lattice relaxation rate is directly related to the value of  $J(\omega)$  at the Larmor frequency of the nucleus. Hence, the relaxation is most effective at the temperature where  $\omega_0 \tau_c \approx 1$ . A minimum value of  $T_1$  is reached at this point.

Because of the highly structured nature and high viscosity of glassy and molten silicates, a broad distribution of correlation times might be expected. Therefore, a superposition of  $J(\omega)$  may be needed to describe the relaxation process, and BPP theory will no longer be strictly valid. In this case, the study of relaxation time can still be quite informative but detailed analysis becomes more difficult. However, one can still use the simple theory as an approximation to draw at least qualitative conclusions. One feature of network liquids such as  $\text{NaAlSi}_3\text{O}_8$  that may tend to simplify its behavior, is the observation that stress and viscous relaxation in these system can usually be characterized by single correlation time (Angell 1984, Napolitano and Macedo 1968).

The  $^{23}\text{Na}$  nucleus has nuclear spin  $I = 3/2$ , and the interaction of the nuclear quadrupole moment with the electric field gradient (EFG) is usually the dominant source of relaxation. The fluctuations of the EFG arise from the diffusive motion of the sodium ions. The spin-lattice relaxation time with the quadrupole mechanism, in the rapid correlation limit (i.e. on the high temperature side of the  $T_1$  minimum where  $\omega_0 \tau_c \ll 1$ ), is given (Abragam 1961) by

$$\frac{1}{T_1} = \frac{3}{40} \frac{2I+3}{I^2(2I-1)} \left[ 1 + \frac{\eta'^2}{3} \right] \left[ \frac{(1-\gamma_\infty)e^2 q Q}{\hbar} \right]^2 \tau_c, \quad (2)$$

where  $\eta'$  is the asymmetry parameter,  $e$  is the electron charge,  $eQ$  is the quadrupole moment of the nucleus,  $(1-\gamma_\infty)eq$  is the electric field gradient at the nucleus, and  $\gamma_\infty$  is called the Sternheimer antishielding factor (Sternheimer and Foley 1956). The factor  $(1-\gamma_\infty)$  arises from the polarization of the electron shells induced by the surrounding ions. For  $\text{Na}^+$ , Sternheimer and Foley (1956) found  $(1-\gamma_\infty) \sim 5$ , in close agreement with the calculation done by Das and Bersohn (1956) using the same model. The collective term  $(e^2 q Q/\hbar)$  is known as the quadrupole coupling constant.

Using the results from relaxation data for  $\text{NaKSi}_2\text{O}_5$  melt (Liu et al., submitted) where a  $^{23}\text{Na}$   $T_1$  minimum was observed,  $T_1 \cong 2 \times 10^{-5}$  s at the minimum, and the quadrupole coupling constant can be evaluated. At  $T_1$  minimum,  $\tau_c \sim 1/\omega_0 \sim 3 \times 10^{-9}$  s for  $^{23}\text{Na}$  is expected. From equation (2), assuming  $\eta' = 0$ , the quadrupole coupling constant  $(e^2 q Q/\hbar) \sim 2.6 \times 10^6$  s $^{-1}$  results. Using this value, the correlation time of Na motion in albite liquid can then be estimated with equation (2). For  $^{23}\text{Na}$  relaxation near the melting point of albite,  $T_1 \sim 7 \times 10^{-4}$  s, and the estimated value of  $\tau_c$  is  $8.5 \times 10^{-11}$  s. A similar calculation at  $T_g$ , where

$T_1 \sim 7.6 \times 10^{-5}$  s, gives a value of  $\tau_c \sim 7.8 \times 10^{-10}$  s. The values of  $\tau_c$  given from the  $^{23}\text{Na}$   $T_1$  data reveal that they are approaching the expected  $T_1$  minimum: extrapolation downward to the point at which  $\omega_0 \tau_c = 1$  predicts the minimum should be at about 883 K.

To the best of our knowledge, similar calculations of  $\tau_c$  cannot be found elsewhere for silicate melts. However, our results can be compared with a  $^{23}\text{Na}$  relaxation study of molten  $\text{NaNO}_3$ . Using a value of  $(e^2 q Q/\hbar) \sim 3.1 \times 10^6$  s $^{-1}$ , Filho et al. (1982) reported  $\tau_c \sim 7.9 \times 10^{-13}$  s for Na translational diffusion in molten  $\text{NaNO}_3$  near the melting point (582 K), in good agreement with the  $\tau_c$  value obtained by Harold-Smith (1973). We note that these types of calculations can only provide a first-order estimation of  $\tau_c$ ; it was found, for example, from NMR spectroscopic analysis of single crystal of  $\text{NaNO}_3$  that the term  $(1-\gamma_\infty)e^2 q Q/\hbar$  decreases from  $2.2 \times 10^6$  s $^{-1}$  at low temperature to  $\sim 2 \times 10^5$  s $^{-1}$  near its melt (Harold-Smith 1973). In contrast, we obtain a much larger value of  $(1-\gamma_\infty)e^2 q Q/\hbar \approx 1.3 \times 10^{-7}$  s $^{-1}$  directly from our  $\text{NaKSi}_2\text{O}_5$   $T_1$  data (Liu et al., submitted). If we take the value for  $\text{NaNO}_3$  and fitted to the  $^{23}\text{Na}$   $T_1$  data for albite near the melting point, the resulting  $\tau_c \sim 3.6 \times 10^{-7}$  s cannot explain the data reported here: the  $^{23}\text{Na}$   $T_1$  data of albite is on the high temperature side of  $T_1$  minimum, and hence must satisfy the condition  $\omega_0 \tau_c \ll 1$ .

In a formal theory of quadrupole relaxation, the electric field gradient at a nucleus located at the origin should depend on the charge and relative distance of all other ions in the sample. But since glasses do not have long range order, the sum over the EFG contributions from all the surrounding ions is difficult to calculate. However, by assuming the quadrupole coupling constant obtained from  $\text{NaKSi}_2\text{O}_5$  liquid is correct, the ionic separation can be estimated to first-order by the relation:  $(1-\gamma_\infty)eq = 2(1-\gamma_\infty)e d^{-3}$  (Filho et al. 1982), where  $d$  is the nearest neighbor distance. Given  $e^2 q Q/\hbar \sim 2.6 \times 10^6$  s $^{-1}$  and  $Q \approx 1.45 \times 10^{-25}$  cm $^2$  (Becker 1980), one obtains  $d = 2.9$  Å. This is closer than typical Na–Na distances in framework silicates, but may be reasonable for a “jump” distance for diffusing Na cations. Values for average Na–Na distances obtained from molecular dynamics simulations of silicate melts are typically also about 3 Å (e.g. Soules and Varshneya 1981), in good agreement with the separation predicted here. For comparison, in molten  $\text{NaNO}_3$  close to the melting temperature, x-ray diffraction data gave  $d = 2.4$  Å (Harold-Smith 1973).

Other possible mechanisms for  $^{23}\text{Na}$  relaxation may arise from paramagnetic impurities or nuclear dipole-dipole interactions. But calculations (Liu et al., submitted) have confirmed that they are too weak to account for the  $^{23}\text{Na}$   $T_1$  data.

The experimental value of  $E_a = 71 \pm 3$  kJ/mol is very close to the activation energy obtained from electric conductivity data of  $E_a \sim 67$  kJ/mol (Jambon and Carron 1976). Self-diffusion of Na measured by the same authors gave a value  $E_D = 57 \pm 12$  kJ/mol, which seems to be significantly lower. However, it was found (Jambon and Semet 1978) that  $E_D$  for  $\text{Na}^+$  diffusion is smaller than that for  $\text{Li}^+$ ,  $\text{K}^+$ ,  $\text{Rb}^+$ , and  $\text{Cs}^+$  diffusion in glass of albite composition, in contrast to the results in  $\text{KAlSi}_3\text{O}_8$  glass, where the activation energies for  $\text{Li}^+$ ,  $\text{Na}^+$ , and  $\text{K}^+$  diffusion are roughly equal. The Na data for albite thus seem somewhat anomalous. Hence,  $^{23}\text{Na}$  relaxation data observed

here reflects the motion that also causes bulk diffusion. Although local "rattling" motions may also exist, and may be important at lower temperature, their frequencies are probably too high to have an important contribution to the  $^{23}\text{Na}$  relaxation (Jain et al. 1985). At lower temperatures, apparent activation energies for spin-lattice relaxation of alkali cations in silicate and borate glasses are indeed reduced, falling to values as low as about 50 percent of those for diffusion (Liu et al., submitted, Jain et al. 1985). This change in behavior may be related to models proposed recently (Ngai and Jain 1986) which involve coupling among diffusing species.

The  $^{23}\text{Na}$   $T_1$  anomaly that occurs near  $T_g$  is a small but reproducible effect. The form of the anomaly indicates that above  $T_g$ , some component of the Na motion is decreased in frequency, increasing the efficiency of relaxation and lowering  $T_1$ . A cooperative type of motion, where  $\text{Na}^+$  is temporarily part of a slowly moving silicate group, could be responsible for this effect.

The offset between  $T_1$  and  $T_2$  data in Figure 1 is not understood. In typical non-viscous liquids, quadrupole relaxation in the extreme narrowing limit should result in  $T_1 = T_2$ . The experimental results report here give  $T_1/T_2 \sim 2$ .

We now turn to the discussion of  $^{29}\text{Si}$  relaxation. As mentioned earlier, measurements of spin-lattice relaxation times in albite and other alkali silicate glass reveal that  $^{29}\text{Si}$   $T_1$  minima occur at temperatures several hundred degrees higher than those for the  $^{23}\text{Na}$ . This strongly suggests that the motion responsible for Si relaxation is not the same as the Na diffusive motion and is probably related to the local motion of the less mobile network forming cation (Si).

One possible mechanism that can contribute to the  $^{29}\text{Si}$  relaxation is the *chemical shift anisotropy* (CSA) interaction. For axial site symmetry in molecules randomly tumbling in a liquid, the following holds (Spiess 1978):

$$\frac{1}{T_1} = \frac{2}{15} \omega_0^2 (\Delta\sigma)^2 \frac{\tau_c}{[1 + \omega_0^2 \tau_c^2]} \quad (3)$$

where  $\omega_0 = \gamma H_0$  is the Larmor frequency in angular frequency unit and  $\Delta\sigma$  is the range of chemical shifts caused by a change in orientation with respect to the magnetic field ( $H_0$ ). Such a simple picture cannot be correct in detail for a framework silicate melt. However, random fluctuations in the bond angles and distances around a silicon atom in a melt could lead to an analogous relationship: the significant factor is the range in resonant frequencies that are "seen" by a nucleus as it and its neighbors move relative to one another.

Since all  $^{29}\text{Si}$   $T_1$  data for liquid  $\text{NaAlSi}_3\text{O}_8$  are at temperatures below the  $T_1$  minimum, an estimate of correlation time at the minimum ( $\tau_c = 1/\omega_0 \sim 4.5 \times 10^{-9}$  s) should be greater than all  $\tau_c$  values for the observed data.  $T_1$  calculated at this point, using equation (3), should thus be *less* than expected values for the real data, if the CSA mechanism dominates relaxation and the parameters chosen are correct.

The CSA for  $^{29}\text{Si}$  in crystalline tectosilicates is generally quite small because of nearly tetrahedral symmetry of the Si sites. The maximum *static* value of the CSA in the present liquid sample must be less than the observed linewidth at low temperatures when motion is too slow to cause line-narrowing. The observed value of  $\Delta\sigma$  is about 3400 Hz or 96 ppm, which results in a calculated  $T_1$  of 7 s at the mini-

mum. This is a factor of about 15 higher than the lowest value observed at the highest temperature.

This discrepancy could be the result of the inappropriateness of equation (3) in a viscous system which may have a complicated distribution of correlation times. Perhaps more likely, however, is a mechanism which can increase the CSA ( $\Delta\sigma$ ) term in equation (3) by  $15^{1/2} = 3.9$ . Flow in the liquid requires the breaking and re-forming of the Si-O bonds. This is reflected in the chemical exchange that is required to produce single, narrow  $^{29}\text{Si}$  NMR lines (Stebbins et al. 1985, Liu et al., submitted), and almost certainly requires the formation of short-lived, highly distorted sites. Short-lived, extreme excursions of the chemical shift would accompany such distortions. A total range of chemical shift values about three times that observed in any crystalline silicate would be required by equation (3), but this could be produced by bond distance changes of perhaps 10-15 percent.

Other mechanisms may also contribute to the Si spin-lattice relaxation. The contribution from the dipole-dipole interaction can be roughly estimated by a calculation of the rigid lattice dipolar linewidth. Again, a strictly accurate calculation of linewidth cannot be obtained because of the uncertain long range structure in a glass. Nevertheless, a first-order approximation can be obtained using the method of Van Vleck (1948) for the second moment ( $M_2$ ) and a few assumptions based on a simplified model. In the absence of motion, the like-spins dipolar second moment for powder samples containing crystallites of random orientations can be written (Abragam 1961) as

$$M_2 = \frac{3}{5} \gamma^4 \hbar^2 I(I+1) \zeta \sum_j R_{ij}^{-6}. \quad (4)$$

The  $\sum R^{-6}$  in the above equation is called the lattice sum and  $\zeta$  is the fractional concentration of the magnetic nuclei. The lattice sum has been evaluated for various structures frequently encountered in molecular solids. Taking a simple cubic structure of lattice constant  $d$ , as a very rough approximate, the lattice sum is  $8.5 d^{-6}$  (Abragam 1961). We consider only the Si-Si like-spin dipolar contribution and neglect the unlike-spin terms that might be present. This is a fairly good approximation because the most likely candidate for unlike-spin dipole interaction is Na-Si; but it is more likely to be averaged out by the much faster motion of Na. If we take  $d = 3.1 \text{ \AA}$ , for the nearest Si-Si separation and  $\zeta = 0.95$ , we get  $M_2 = 3.6 \times 10^6 \text{ (rad/s)}^2$ . Assuming a Gaussian lineshape, the rigid dipolar FWHM linewidth can be calculated from  $M_2$  by (Abragam 1961)  $\Delta f = (1/\pi) [2(\ln 2) M_2]^{1/2} = 712 \text{ Hz}$ . The rigid lattice linewidth calculated from this oversimplified model can then be compared to the experimental rigid linewidth of 1700 Hz, and reflects a  $T_2 = 1/(\pi \Delta f) \sim 4 \times 10^{-4}$  s. Other factors probably also contribute to the  $^{29}\text{Si}$  linewidth. In particular, the isotopic linewidth of albite with natural abundance  $^{29}\text{Si}$  was measured by Murdoch et al. (1985) using the  $^{29}\text{Si}$  MAS technique at room temperature. The integrated linewidth of 18 ppm (corresponding to 640 Hz here) is mainly due to heterogeneous broadening. Furthermore, the contribution from chemical shift anisotropy may also be significant.

In order to investigate the dipolar contribution to the Si spin-lattice relaxation, a calculation similar to that for CSA mechanism will be presented. For isotropic, random molecular motion, the like-spin dipole-dipole contribution to the spin-lattice relaxation can be written (Boden 1979)

as

$$\frac{1}{T_1} = \frac{2}{3} M_2 \left[ \frac{\tau_c}{1 + \omega_0^2 \tau_c^2} + \frac{4\tau_c}{1 + 4\omega_0^2 \tau_c^2} \right]. \quad (5)$$

In this case, the  $T_1$  minimum occurs when  $\omega_0 \tau_c \approx 0.62$ . Taking  $\tau_c \sim 2.8 \times 10^{-9}$  s and using the  $M_2$  value derived earlier, equation (5) gives  $T_1 \sim 65$  s. On the other hand, if we take the observed linewidth of 1700 Hz at low temperature as a maximum estimate of the rigid lattice dipolar linewidth, the resulting  $M_2 \sim 2 \times 10^7$  (rad/s)<sup>2</sup> gives  $T_1 \sim 11$  s using equation (5). Since the observed relaxation rate ( $1/T_1$ ) must be the sum of all contributions, the Si–Si dipolar interaction calculated with these assumptions can play only a minor role. These calculations probably indicate the maximum effect of Si–Si dipolar couplings: recent measurements on both <sup>29</sup>Si enriched and unenriched NaAlSi<sub>3</sub>O<sub>8</sub> glass suggest that the coupling is smaller than a few hundred Hz at room temperature (Stebbins and Liu, in preparation).

The <sup>29</sup>Si  $T_1$  data above  $T_g$  show curvature slightly away from Arrhenius behavior, probably because of an approach to a minimum at higher temperature. If one fits the  $T_1$  data throughout the high temperature range, using equation (1), the activation energy is  $\sim 125$  kJ/mol. The activation energy for viscous flow in albite liquid is  $E_\eta \sim 398$  kJ/mol (Cranmer and Uhlmann 1981), close to the Si–O bond strength of  $\sim 444$  kJ/mol. Hence, the result obtained from our <sup>29</sup>Si  $T_1$  data suggest that the motions responsible for Si diffusion or viscosity are not identical to those which cause spin-lattice relaxation. It is likely that the spin-lattice relaxation is dominated by some kind of local motion, whereas viscous flow (and probably the motional narrowing of <sup>29</sup>Si NMR spectra) involves the cooperative motion of several silicons and oxygens. As in the case of sodium motion, the property involving coupling among species will exhibit the higher activation energy (Liu et al., submitted).

Finally, it is surprising that the last few points of the <sup>29</sup>Si  $T_1$  and <sup>29</sup>Si linewidth measurements seem to have the same temperature dependence as the <sup>23</sup>Na data. Although this behavior may be more than a coincidence, it is not yet understood.

## Conclusions

The first data presented on nuclear relaxation in glassy and liquid NaAlSi<sub>3</sub>O<sub>8</sub> provide suggestions concerning the low-frequency atomic motion that occurs in molten silicates, and how this motion changes at the glass transition.

Spin-lattice relaxation time data show that the entire temperature range studied (about 600 to 1200° C) is above the  $T_1$  minimum for <sup>23</sup>Na, but below the minimum for <sup>29</sup>Si. This confirms the general picture of the relatively high mobility of the alkali cation that has been drawn from studies of bulk transport properties. The activation energy for relaxation of <sup>23</sup>Na is the same as for electrical conductivity, and the relaxation mechanism is probably through quadrupolar interactions coupled through the same type of motion that is responsible for through-going diffusion.

The relaxation mechanism for <sup>29</sup>Si is less certain, but possibly involves the formation of short-lived, distorted sites with extreme chemical shift values. These distortions are presumably produced when the structure becomes mobile above the glass transition. This local mobility is probably an important factor in the “liquid” component of thermodynamic properties, but long-range viscous flow also

probably includes less frequent Si–O bond-breaking events. These are more directly related to the site-exchange mechanism more clearly seen in alkali silicate samples (Stebbins et al. 1985, Liu et al., submitted).

Most importantly, the spin-lattice relaxation mechanism for <sup>29</sup>Si changes dramatically at the bulk glass transition temperature, indicating that relaxation does involve structural motion which begins only when the well-known breaks in thermodynamic properties occur. This may be the first instance in which the changes in configuration that are assumed to begin on heating through  $T_g$  have been linked to local motion of network-forming cations.

The relaxation of <sup>23</sup>Na is slightly perturbed at  $T_g$ , indicating that some “flow events” probably also involve cooperative motion of both network-modifying and network-forming cations.

Several aspects of relaxation and structural motion in molten silicates are seen more completely in new data on alkali silicates (Liu et al., submitted). Complete confirmation of proposed relaxation mechanisms, and their relation to structural mobility, await further measurements, particularly those made at varying frequency.

*Acknowledgements.* We would like to thank M.S. Conradi and G.E. Brown, Jr. for helpful discussions, C.A. Angell for a thoughtful and informative review, and A. Navrotsky for editorial assistance. We acknowledge support from the National Science Foundation, grant number EAR-8507925 (to J.F. Stebbins); and the Director, Office of Energy Research, Office of Basic Energy Sciences, Material Sciences Division of the U.S. Department of Energy under contract No. DE-AC03-76F00098; and the Stanford School of Earth Sciences.

## References

- Abragam A (1961) Principles of nuclear magnetism. Oxford University Press, Oxford London
- Adam G, Gibbs JH (1965) On the temperature dependence of cooperative relaxation properties in glass-forming liquids. *J Chem Phys* 43:139–146
- Angell CA (1984) Strong and fragile liquids. Relaxations in Complex Systems. Ngai KL and Wright GB (eds) Office of Naval Research and National Technical Information Service
- Arndt J, Haberle F (1973) Thermal expansion and glass transition temperatures of synthetic glasses of plagioclase-like compositions. *Contrib Mineral Petrol* 39:175–183
- Aurora TS, Day SM (1982) High-temperature NMR probe. *Rev Sci Instr* 53:1152–1154
- Becker ED (1980) High resolution NMR – theory and chemical applications, second edition, Academic Press, NY, Appendix B
- Bloembergen N, Purcell EM, Pound RV (1948) Relaxation effects in nuclear magnetic absorption. *Phys Rev* 73:679–712
- Boden N (1979) NMR studies of plastic crystals. The plastically crystalline state, (ed) Sherwood JN, John Wiley & Sons, NY
- Boettcher AL, Guo Q, Bohlen SR, Hanson B (1984) Melting in feldspar-bearing systems to high pressures and the structure of aluminosilicate liquids. *Geology* 12:202–204
- Brawer S (1985) Relaxation in viscous liquids and glasses. The American Ceramic Society Inc., Columbus Ohio
- Cranmer D, Uhlmann DR (1981) Viscosity of liquid albite, a network material. *J Non-Cryst Solids* 45:283–288
- Das TP, Bersohn R (1956) Variational approach to the quadrupole polarizability of ions. *Phys Rev* 102:733–738
- Eisenberg D, Kauzmann W (1969) The structure and properties of water. Oxford University Press, Oxford London
- Farrar TC, Becker ED (1971) Pulse and Fourier Transform NMR. Academic Press, New York

- Filho WW, Havill RL, Titman JM (1982) Nuclear spin relaxation in molten alkali nitrates. *J Magn Reson* 49:296–303
- Furukawa T, White WB (1981) Raman spectroscopy of heat-treated  $B_2O_3-SiO_2$  glasses. *J Am Chem Soc* 64:443–447
- Fyfe CA (1983) Solid state NMR for chemists. CFC Press, Guelph Ontario Canada
- Gibbs JH, DiMarzio EA (1958) Nature of the glass transition and the glassy state. *J Chem Phys* 28:373–383
- Hahn EL (1950) Spin echoes. *Phys Rev* 80:580–594
- Harold-Smith D (1973) Nuclear magnetic relaxation in molten salts. I. spin-lattice relaxation time of  $^{23}Na$  in molten sodium nitrate. *J Chem Phys* 59:4771–4777
- Jain H, Balzer-Jollenbeck G, Kanert O (1985)  $^7Li$  nuclear magnetic resonance in ( $^7Li$ ,  $^6Li$ ) and (Li, Na) triborate glasses. *J Am Ceram Soc* 68:C24–C26
- Jambon A, Carron J-P (1976) Diffusion of Na, K, Rb and Cs in glasses of albite and orthoclase composition. *Geochim Cosmochim Acta* 40:897–903
- Jambon A, Semet MP (1978) Lithium diffusion in silicate glasses of albite, orthoclase, and obsidian composition: an ion-microprobe determination. *Earth Planet Sci Lett* 37:445–450
- Kirkpatrick RJ, Kinsey RA, Smith KA, Henderson DM, Oldfield E (1985) High resolution solid state sodium-23, aluminum-27, and silicon-29 nuclear magnetic resonance spectrographic reconnaissance of alkali and plagioclase feldspars. *Am Mineral* 70:106–123
- McKeown DA, Galeener FL, Brown GE (1984) Raman studies of Al coordination in silica-rich sodium aluminosilicate glasses and some related minerals. *J Non-Cryst Solids* 68:361–378
- McKeown DA, Waychunas GA, Brown GE (1985a) EXAFS and XANES study of the local coordination environment of sodium in a series of silica-rich glasses and selected minerals within the  $Na_2O-Al_2O_3-SiO_2$  system. *J Non-Cryst Solids* 74:325–348
- McKeown DA, Waychunas GA, Brown GE (1985b) EXAFS study of the coordination environment of aluminum in a series of silica-rich glasses and selected minerals within the sodium aluminosilicate system. *J Non-Cryst Solids* 74:349–360
- McMillan PF, Piriou B, Navrotsky A (1982) A Raman spectroscopic study of glasses along the joins silica-calcium aluminate, silica-sodium aluminate, and silica-potassium aluminate. *Geochim Cosmochim Acta* 46:2021–2037
- Murdoch JB, Stebbins JF, Schneider E, Carmichael ISE (1984) NMR spectroscopy of Si-29, Na-23, and Al-27 in molten silicates to 1300°C: approach and spectra. *Trans Am Geophys Union* 65:1141
- Murdoch JB, Stebbins JF, Carmichael ISE (1985) High-resolution  $^{29}Si$  NMR study of silicate and aluminosilicate glasses: the effect of network-modifying cations. *Am Mineral* 70:332–343
- Mysen BO, Virgo D, Scarfe CM (1980) Relations between the anionic structure and viscosity of silicate melts – a Raman spectroscopic study. *Am Mineral* 65:690–710
- Mysen BO, Virgo D, Kushiro I (1981) The structural role of aluminum in silicate melts – a Raman spectroscopic study at one atmosphere. *Am Mineral* 66:678–701
- Napolitano A, Macedo PB (1968) Spectrum of relaxation times in  $GeO_2$  glass. *J Res Nat Bur Stand* 72A:425–433
- Navrotsky A, Peraudeau G, McMillan P, Coutures J (1982) A Thermochemical study of glasses and crystals along the joins silica-calcium aluminate and silica-sodium aluminate. *Geochim Cosmochim Acta* 46:2039–2047
- Neil JM, Apps JA (1979) Solubility of albite in the aqueous phase at elevated temperatures. Lawrence Berkeley Laboratory report LBL-10349
- Ngai KL, Jain H (1986) Conductivity relaxation and spin lattice relaxation in lithium and mixed alkali borate glasses: activation enthalpies, anomalous isotope-mass effect and mixed alkali effect. *Solid State Ionics* 18&19:362–367
- Ploumbidis D (1979) A high-temperature and high-field nuclear magnetic resonance instrument. *Rev Sci Inst* 50:1133–1135
- Rammensee W, Fraser DG (1982) Determination of activities in silicate melts by Knudsen cell mass spectroscopy – I. The system  $NaAlSi_3O_8-KAlSi_3O_8$ . *Geochim Cosmochim Acta* 46:2269–2278
- Richet P, Bottinga Y (1983) Glass transitions and thermodynamic properties of amorphous  $SiO_2$ ,  $NaAlSi_nO_{2n+2}$ , and  $KAlSi_3O_8$ . *Geochim Cosmochim Acta* 48:453–470
- Richet P (1984) Viscosity and configurational entropy of silicate melts. *Geochim Cosmochim Acta* 48:471–483
- Richet P, Robie RA, Hemingway BS (1986) Low temperature heat capacity of diopside glass –  $CaMgSi_2O_6$ : a calorimetric test of the configurational entropy theory applied to the viscosity of the liquid silicate. *Geochim Cosmochim Acta* 50:1521–1534
- Schneider E (1985) Application of high resolution NMR to Geochemistry: crystalline, glassy, and molten silicates. Ph.D. thesis, Department of Chemistry, University of California, Berkeley, and Lawrence Berkeley Laboratory report LBL-20936
- Seifert F, Mysen BO, Virgo D (1982) Three-dimensional network structure in quenched melts (glasses) in the system  $SiO_2-AlO_2$ ,  $SiO_2-CaAl_2O_4$ , and  $SiO_2-MgAl_2O_4$ . *Am Mineral* 67:696–717
- Sharma SK, Virgo D, Mysen BO (1978a) Structure of melts along the join  $SiO_2-NaAlSiO_4$  by Raman spectroscopy. *Carnegie Inst Wash Year Book* 77:652–658
- Sharma SK, Virgo D, Mysen BO (1978b) Structure of glasses and melts of  $Na_2O-xSiO_2$  ( $x=1, 2, 3$ ) composition from Raman spectroscopy. *Carnegie Inst Wash Year Book* 77:649–652
- Slichter CP (1980) Principles of magnetic resonance. Springer-Verlag, Berlin Heidelberg New York
- Soller FX, Sotier S, Coufal H, Hackstein K (1979) A high-temperature furnace for NMR measurements. *J Phys E: Sci Inst* 12:577–579
- Soules TF, Varshneya AK (1981) Molecular dynamic calculations of a sodium borosilicate glass structure. *J Am Ceram Soc* 64:145–150
- Spieß HW (1978) Rotation of molecules and nuclear spin relaxation. NMR basic principles and progress, Vol. 15, Diehl P, Fluck E, Kosfeld R (eds) Springer-Verlag, New York
- Stebbins JF, Carmichael ISE, Weill DF (1983) The high temperature liquid and glass heat constants and the heats of fusion of diopside, albite, sanidine, and nepheline. *Am Mineral* 68:717–730
- Stebbins JF, Murdoch JB, Schneider E, Carmichael ISE, Pines A (1985) A high-temperature high-resolution NMR study of  $^{23}Na$ ,  $^{27}Al$  and  $^{29}Si$  in molten silicates. *Nature* 314:250–252
- Stebbins JF, Schneider E, Murdoch JB, Pines A, Carmichael ISE (1986) A new probe for high-temperature nuclear magnetic resonance spectroscopy with ppm resolution. *Rev Sci Inst* 57:39–42
- Sternheimer RM, Foley HM (1956) Nuclear quadrupole coupling in polar molecules. *Phys Rev* 102:731–732
- Taylor M, Brown GE (1979) Structure of mineral glasses-I. The feldspar glasses  $NaAlSi_3O_8$ ,  $KAlSi_3O_8$ ,  $CaAl_2Si_2O_8$ . *Geochim Cosmochim Acta* 43:61–75
- Urbain G, Bottinga Y, Richet P (1982) Viscosity of silica, silicates, and aluminosilicates. *Geochim Cosmochim Acta* 46:1061–1072
- Van Vleck JH (1948) The dipolar broadening of magnetic resonance lines in crystals. *Phys Rev* 74:1168–1183
- Waseda Y (1980) The structure of non-crystalline materials. McGraw-Hill, New York

Received February 27, 1987